Interaction and Multiscale Mechanics, *Vol. 6, No. 4 (2013) 339-356*
DOI: http://dx.doi.org/10.12989/imm.2013.6.4.339

ABC optimization of TMD parameters for tall buildings with soil structure interaction

Anooshiravan Farshidianfar* and Saeed Soheili[a]

Department of Mechanical Engineering, Ferdowsi University of Mashhad, Vakilabad Blvd., Mashhad, Iran

(Received October 23, 2013, Revised November 1, 2013, Accepted November 11, 2013)

Abstract. This paper investigates the optimized parameters of Tuned Mass Dampers (TMDs) for vibration control of high-rise structures including Soil Structure Interaction (SSI). The Artificial Bee Colony (ABC) method is employed for optimization. The TMD Mass, damping coefficient and spring stiffness are assumed as the design variables of the controller; and the objective is set as the reduction of both the maximum displacement and acceleration of the building. The time domain analysis based on Newmark method is employed to obtain the displacement, velocity and acceleration of different stories and TMD in response to 6 types of far field earthquakes. The optimized mass, frequency and damping ratio are then formulated for different soil types; and employed for the design of TMD for the 40 and 15 story buildings and 10 different earthquakes, and well results are achieved. This study leads the researchers to the better understanding and designing of TMDs as passive controllers for the mitigation of earthquake oscillations.

Keywords: Tuned Mass Damper (TMD); Soil-Structure Interaction (SSI); Artificial Bee Colony (ABC); Curve Fitting.

1. Introduction

In the last decades, tall buildings are widely developed and employed in most countries. These structures are generally flexible and possess low damping properties. They are usually subjected to the earthquake vibrations. Therefore, the study of tall buildings for vibration mitigation using various absorbers has attracted the interest of many researchers. Moreover, it is realized that the soil characteristics and the interaction between soil and structure greatly influence the structural responses.

A tuned mass damper (TMD) is a kind of vibration absorber consisting of mass, spring and viscous damper attached to the vibrating system to mitigate oscillations. It passively dissipates energy through the interaction of inertial force produced by mass movement and the damping effects induced by dampers.

As Ormondroyd and Den Hartog (1928) mentioned, the application of TMD was firstly proposed in 1909. Since then, many theoretical and experimental researches have been performed to study the TMDs mechanism of vibration mitigation and their application to structures. The

*Corresponding author, Professor, E-mail: farshid@um.ac.ir
[a]Ph.D. Student, E-mail: soheili78@yahoo.com

http://www.techno-press.org/?journal=imm&subpage=7 ISSN: 1976-0426 (Print), 2092-6200 (Online)

TMDs are usually installed on the top floor, and several researches have been conducted to study their effectiveness for earthquake (Miyama 1992) and wind (Kawaguchi *et al*. 1992, Tsukagoshi *et al*. 1993) excitations.

Gupta *et al*. (1969) investigated the effects of several TMDs with elastic-plastic properties on the response of single degree of freedom structures subjected to the Kern County earthquake (1952). To investigate the effect of TMDs on the fundamental mode response, Kaynia *et al*. (1981) studied the optimum reduction of structures response subjected to 48 earthquake spectra. They figured out that the TMDs are less effective in decreasing the response of structures than previously thought. Sladek and Klingner (1983) investigated the best parameters of a TMD placed on top floor of a 25 story building, based on the minimization of response to sinusoidal loadings.

An optimization method is employed by Wirsching and Campbell (1974) to calculate the TMD parameters for 1-, 5- and 10-story buildings. According to their study, TMDs are effective devices in reducing response. Ohno *et al*. (1977) presented optimized TMD parameters based on the minimization of mean square acceleration response to earthquake excitations. Several studies on the application of the TMD and its best values are performed by other researchers such as Villaverde *et al*. (1994). Later, Sadek *et al*. (1997) presented some formulations for computing the optimal parameters of TMD device based on equal damping for the first two modes of system.

Considering soil effects, the structure response differs from the fixed base model. The oscillation energy is actually transferred to the soil through the foundation. Therefore, the soil and structure influence each other, which is called the soil-structure interaction (SSI). Various investigations are performed to study the SSI effects. For example, frequency domain analysis was performed by Xu and Kwok (1992) to obtain the wind induced vibrations of soil-structure-damper system. Moreover, frequency independent expressions were presented by Wolf (1994) to determine the swaying and rocking dashpots, and the related springs of a rigid circular foundation. Recently, Liu *et al*. (2008) developed a mathematical model for time domain analysis of wind induced oscillations of a tall building with TMD considering the soil effects.

Multiple Tuned Mass Damper (MTMD) is another mechanism employed for reducing the earthquake induced vibration of structures, which consists of different mass-spring systems with tuned frequencies. The study of MTMD effect on the vibration control of torsionally coupled structures with SSI effects by Wang and Lin (2005) shows that both the SSI and eccentricity effects should be considered for determination of optimal MTMD parameters to avoid overestimation of its effectiveness. Lin *et al*. (2010) investigated the influence of active control system for an irregular building. They concluded that the SSI effect is significant for both squatty and slender buildings, therefore; the soil structure interaction should be considered for the design of active control devices especially for high-rise buildings.

Li *et al*. (2010) studied the effects of various parameters in the soil-asymmetric structure interaction system on both the effectiveness and robustness of the active TMD and MTMD. Li (2012) indicated that when an asymmetric structure is built on soft soil sites, the effectiveness and robustness of the active MTMD for asymmetric structures is underestimated or overestimated if the SSI effect is disregarded. According to Li and Han (2011), the dominant ground frequency and soil characteristics have significant effects on the effectiveness, optimum parameters and stroke displacement of the MTMD.

Although numerous works are performed concerning the SSI effects, few investigations were carried out on the time response of high-rise buildings due to earthquake excitations. In fact, the earthquake time response of tall buildings has usually been calculated employing fixed base models. These analyses cannot reasonably predict the structural responses. Moreover, the optimal parameters of 3 TMD are extremely related to the soil type. Therefore, the time domain analysis of structures including the SSI effects is an advantageous process for better understanding of earthquake oscillations and TMD devices. Furthermore, few works have considered and employed heuristic algorithms, among which the Artificial Bee Colony (ABC) method can be effectively employed for the optimized design of TMDs.

In this paper, a mathematical model is developed for calculating the earthquake response of a high-rise building with TMDs as passive controller. The model is employed to obtain the time response of 40 story buildings using TMDs. The heuristic methods are applied on the model to obtain the best TMD parameters. Three different soil types, namely soft, medium and dense soils together with the fixed base model are investigated. The results are then employed for the modification of the previous relations to achieve the best TMD parameters considering the SSI effects. The relations are then employed to calculate the 40 and 15 story structures with 10 new earthquakes.

2. Modeling of tall buildings

Fig. 1 shows an N-story structure with a TMD and the SSI effects considered. Mass and moment of inertia for each floor are indicated as M_i and I_i , and those of foundation are shown as M_0 and I_0 , respectively. The stiffness and damping between floors are assumed as K_i and C_i , respectively. M_{TMD} , K_{TMD} and C_{TMD} are the related parameters for TMD. Damping of the swaying and rocking dashpots are represented as C_s and C_r , and the stiffness of the corresponding springs are indicated as K_s and K_r , respectively. The time histories of displacement and rotation of foundation are respectively defined as X_0 and θ_0, and the displacement of each story is shown as X_i. The height of each floor is also assumed as Z_i.

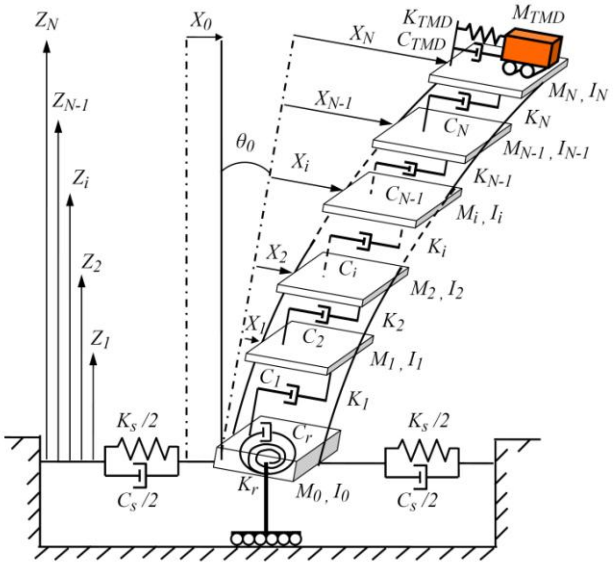

Fig. 1 Shear building configuration

Using Lagrange's equation, the equation of motion for the building shown in Fig. 1 can be represented as follows (Thomson and Dahleh 1997)

$$[m]\{\ddot{x}(t)\}+[c]\{\dot{x}(t)\}+[k]\{x(t)\}=-[m^{*}]\{1\}\ddot{u}_g \tag{1}$$

where $[m]$, $[c]$ and $[k]$ denote the mass, damping and stiffness of the oscillating system. $[m^*]$ indicates the acceleration mass matrix for earthquake and $\ddot{u}_g$ is the earthquake acceleration. Considering the SSI effects, the N-story structure is a $N + 3$ degree-of-freedom oscillatory system. For such a building, the mass, damping and stiffness matrices are obtained by employing Lagrange's equation in the following form (Thomson and Dahleh 1997, Liu *et al*. 2008)

$$[m]=\begin{bmatrix} [M]_{N\times N} & \{0\}_{N\times 1} & [M]_{N\times 1} & [MZ]_{N\times 1} \\ & M_{TMD} & M_{TMD} & M_{TMD}Z_N \\ & & M_0+\sum_{j=1}^{N}M_j+M_{TMD} & \sum_{j=1}^{N}M_jZ_j+M_{TMD}Z_N \\ symmetry & & & I_0+\sum_{j=1}^{N}(I_j+M_jZ_j^2)+M_{TMD}Z_N^2 \end{bmatrix} \tag{2a}$$

$$[k]=\begin{bmatrix} [K]_{N\times N} & \{K_{TMD}\}_{N\times 1} & \{0\}_{N\times 1} & \{0\}_{N\times 1} \\ & K_{TMD} & 0 & 0 \\ & & K_s & 0 \\ symmetry & & & K_r \end{bmatrix} \tag{2b}$$

$$[c]=\begin{bmatrix} [C]_{N\times N} & \{C_{TMD}\}_{N\times 1} & \{0\}_{N\times 1} & \{0\}_{N\times 1} \\ & C_{TMD} & 0 & 0 \\ & & C_s & 0 \\ symmetry & & & C_r \end{bmatrix} \tag{2c}$$

$$[m^{*}]=\begin{bmatrix} [M]_{N\times N} & \{0\}_{N\times 1} & \{0\}_{N\times 1} & \{0\}_{N\times 1} \\ 0 & M_{TMD} & 0 & 0 \\ 0 & 0 & M_0+\sum_{j=1}^{N}M_j+M_{TMD} & 0 \\ 0 & 0 & \sum_{j=1}^{N}M_jZ_j+M_{TMD}Z_N & 0 \end{bmatrix} \tag{2d}$$

Ignoring the SSI effects, means that the rows and columns $N + 2$ and $N + 3$ are neglected; and the mentioned matrices are reduced to $(N + 1) \times (N + 1)$ dimensional matrices.

Using the Rayleigh proportional damping, the damping matrix of N-story structure can be represented as follows

$$[c]_{N\times N}=A_0[m]_{N\times N}+A_1[k]_{N\times N} \tag{3}$$

in which A_0 and A_1 are the Rayleigh damping coefficients.

The displacement vector $\{x(t)\}$ including both the displacement and rotation of the floors and foundation as well as the TMD motion can be represented as follows

$$\{x(t)\} = \{X_1(t) \quad X_2(t) \quad ... \quad X_N(t) \quad X_{TMD}(t) \quad X_0(t) \quad \theta_0(t)\}^T \tag{4}$$

The parameters C_s , C_r , K_s and K_r can be obtained from the soil properties (i.e., poisson's ratio v_s , density ρ_s , shear wave velocity V_s and shear modulus G_s) and radius of foundation R_0 (Liu *et al*. 2008).

In this paper, various earthquake acceleration spectra are applied to the structure, and the time response of the TMD and building are calculated based on Newmark's integration method (Newmark 1959).

3. Artificial Bee Colony (ABC) method

The natural behavior of bees and their collective activities in their hives have fascinated researchers for centuries. Several algorithms have been proposed and developed based on the foraging behavior of bees. Regarding combinatorial optimization, the works of Tereshko and Leongarov (2005) are leading. They modeled robots as bees having limited intelligence individually, but their cooperative behavior makes real robotic tasks possible. For optimization in continuous domains, Yang developed a method called Virtual Bee Algorithm (VBA) which was applied to optimizing benchmark functions with a maximum dimension of two (Yang 2005). Artificial Bee Colony (ABC) algorithm, the method employed in this paper, was presented by Karaboga (2005) to optimize numeric benchmark functions. It was then extended by Karaboga and Basturk and showed to outperform other recognized heuristic methods such as GA (Basturk and Karaboga 2006) and DE, PSO and EA (Basturk and Karaboga 2008).

Similar to other nature-based algorithms, ABC models honey bees but not necessarily precisely. In this model, the honey bees are categorized as employed, onlooker and scout. An employed bee is a forager associated with a certain food source which she is currently exploiting. She memorizes the quality of the food source and then after returning to the hive, shares it with other bees waiting there via a peculiar communication called waggle dance. An onlooker bee is an unemployed bee at the hive which tries to find a new food source using the information provided by employed bees. A scout, ignoring the other's information, searches around the hive randomly. In nature, the employment of unemployed bees happens in a nearly similar way. In addition, when the quality of a food source is below a certain level, it will be abandoned to make the bees explore for new food sources.

In ABC, the solution candidates are modeled as food sources and their corresponding objective functions as the quality (nectar amount) of the food source. For the first step, the artificial employed bees are randomly scattered in the search domain producing *SN* initial solutions. Here, *SN* represents the number of employed or onlooker bees which are considered equal until the end of algorithm. It is notable that any of these solutions x_i (i =1, 2…, *SN*) is a *D*-dimensional vector representing *D* design variables constructing the objective function. After this initialization, the main loop of the algorithm described hereafter is repeated for a predetermined number of cycles or until a termination criterion is satisfied.

Firstly, all employed bees attempt to find new solutions in the neighbor of the solution (food source) they memorized at the previous cycle. If the quality (the amount of objective function) is higher at this new solution, then she forgets the former and memorizes the new one. In ABC, a particular mechanism is devised for this purpose; which only allows one of the dimensions of the current solution being subject to modification

$$v_{ij} = x_{ij} + \phi_{ij}(x_{ij} - x_{kj}) \tag{5}$$

where $j \in \{1,2,\cdots,D\}$ and $k \in \{1,2,\cdots,SN\}$ are randomly chosen indices, and v_{ij} represents the new solution (new food source position). It should be noted that $k \neq i$. The parameter ϕ_{ij} is also a random number in the domain [-1, 1].

After that, the onlooker bees should select the solution around which they explore for new food sources. This is performed probabilistically i.e., a mechanism like roulette wheel is employed using the fitness (the related objective function or a similar concept) of all current solutions. With the help of a uniform random number generator, the solutions for further exploration can be easily determined

$$p_i = \frac{fit_i}{\sum_{n=1}^{SN} fit_n} \tag{6}$$

Noticeably, some onlooker bees might be directed to search around identical solutions. When the solutions are selected, producing new candidate solutions around them is done the same way the employed bees perform using (5). Additionally, updating food sources is done with the same greedy process by comparing the new solutions produced by onlookers and the corresponding current solutions. It is notable that different approaches have been proposed for assigning fitness to solutions especially when minimization is to be done with an originally maximizing algorithm such as ABC or when negative values of objective function is engaged. Karaboga (2008) has utilized a familiar form described below which is adopted in this paper as well

$$fit_i = \begin{cases} \dfrac{1}{1+f_i} & f_i \geq 0 \\ 1+|f_i| & f_i < 0 \end{cases} \tag{7}$$

where f_i is the objective function of solution x_i .

If a solution can not be improved by employed or onlooker bees after certain iterations called *limit*, then the solution is abandoned and the bee becomes a scout. In that case, the scout bee searches randomly for a new solution within the search space. It should be reminded that at each cycle, only one artificial bee is allowed to become scout and perform the search as follows

$$x_i^j = x_{\min}^j + \varphi(x_{\max}^j - x_{\min}^j) \tag{8}$$

where φ is a random number in domain [0, 1]. Obviously, variables of all dimensions are replaced with new randomly-generated values.

Since the problem is of multi-objective nature concerning minimization of both the maximum displacement and acceleration of the building, an overall objective function including both concepts should be employed. Here, as the acceleration results are nearly 10 times greater than the values of displacement, the objective function is defined as follows

$$f_i = \ddot{u}_{\max} + 10u_{\max} \tag{9}$$

where $u_{\max}$ and $\ddot{u}_{\max}$ denote the maximum displacement and acceleration values, respectively. The flowchart of the ABC algorithm employed for TMD optimization is presented in Fig. 2.

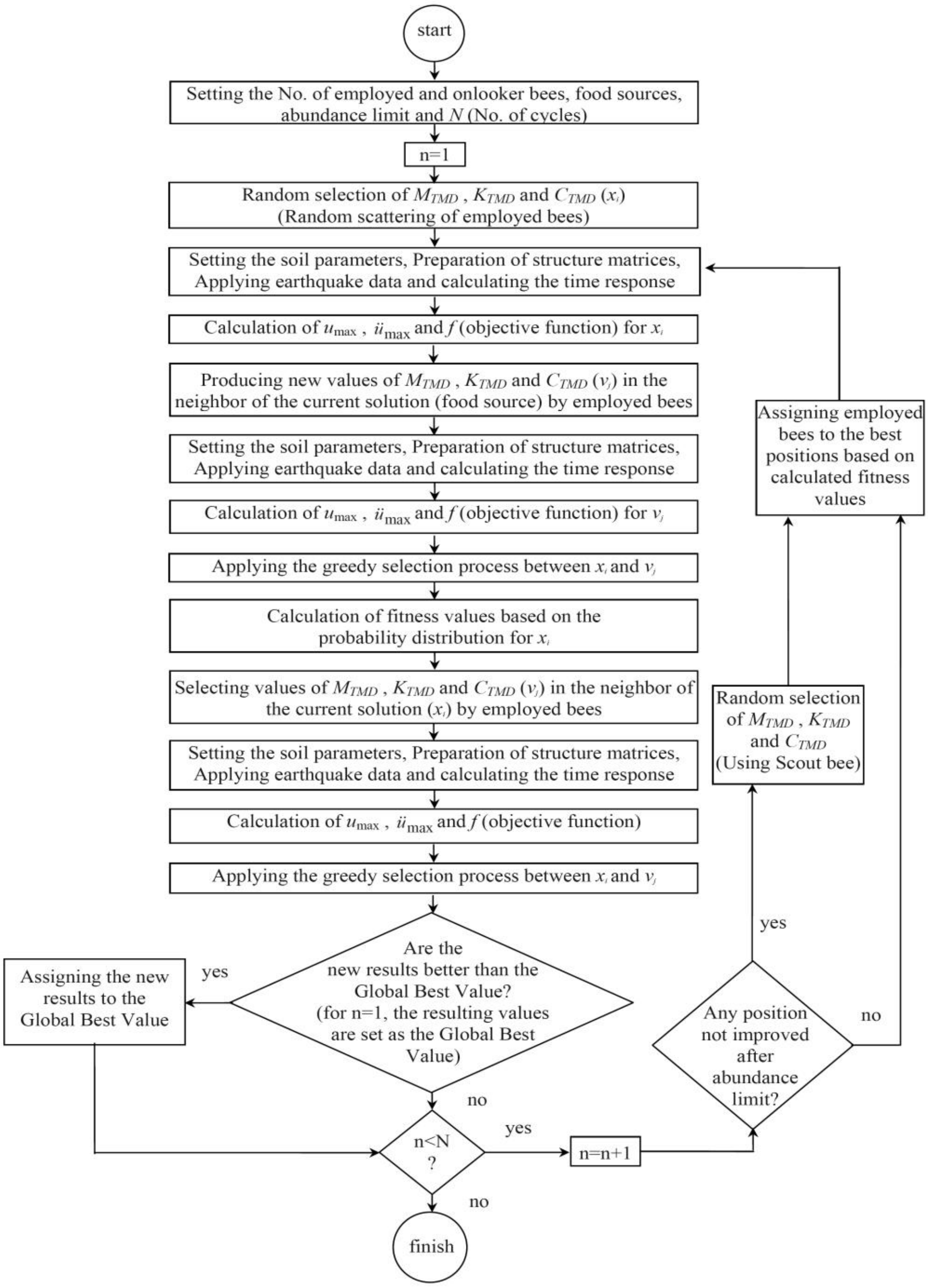

Fig. 2 The flowchart of ABC algorithm for TMD optimization

4. Illustrative example

The methodology outlined previously is employed to calculate the structural response of a 40-story building with a TMD. Table 1 shows the structure parameters (Liu *et al.* 2008). The stiffness K_i linearly decreases as Z_i increases. The TMD is installed on the top of building for the better damping effect of vibrations.

In this study, three types of ground properties, namely soft, medium and dense soil are examined. A structure with a fixed base is also investigated. The soil and foundation properties are presented in Table 2.

Table 3 represents the first 3 natural and damped frequencies of the structure, considering and ignoring the SSI effects. The TMD design variables are set in such a way that all the first 3 frequencies of the structure are covered, and damping ratio (ξ) is always less than unity. In this way, the maximum mass ratio is about 3.5% of the first modal mass, i.e., $50\times10^3 \leq M_{TMD} \leq 1000\times10^3$ (kg), the TMD spring stiffness is set as $0.3\times10^6 \leq K_{TMD} \leq 60\times10^6$ (N/m) and the TMD damping is tuned to $0.1 \times 10^3 \leq C_{TMD} \leq 2000 \times 10^3$ (Ns/m).

As mentioned before, 5 types of far field earthquakes, namely Cape Mendocino, Coalinga, Imperial Valley, Landers, and Loma Prieta earthquake data are employed to obtain the optimized mass ratio (μ), frequency ratio (f) and damping ratio (ξ) for the TMD device, which are defined as follows

$$\mu_{opt} = \frac{M_{TMD}}{M_s} \tag{10}$$

$$f_{opt} = \frac{\omega_{TMD}}{\omega_s} \tag{11}$$

$$\xi_{opt} = \frac{C_{TMD}}{2M_{TMD}\omega_{TMD}} \tag{12}$$

where M_s relates to the first modal mass of structure based on the unit modal participation factor, and ω_s shows the first frequency of the fix based structure.

Table 1 Structure parameters (Liu *et al.* 2008)

No. of stories	40
Story height (Z_i)	4 m
Story mass (M_i)	9.8×10^5 kg
Story moment of inertia (I_i)	1.31×10^8 kgm^2
Story stiffness (K_i)	$K_1=2.13\times10^9$ N/m $K_{40}=9.98\times10^8$ N/m $K_{40} \leq K_i \leq K_1$
Foundation radius (R_0)	20 m
Foundation mass (M_0)	1.96×10^6 kg
Foundation moment of inertia (I_0)	1.96×10^8 kgm^2

Table 2 Parameters of the soil and foundation (Liu *et al.* 2008)

Soil Type	Swaying damping C_s (Ns/m)	Rocking damping C_r (Nsm)	Swaying stiffness K_s (N/m)	Rocking stiffness K_r (N/m)
Soft Soil	2.19×10^8	2.26×10^{10}	1.91×10^9	7.53×10^{11}
Medium Soil	6.90×10^8	7.02×10^{10}	1.80×10^{10}	7.02×10^{12}
Dense Soil	1.32×10^9	1.15×10^{11}	5.75×10^{10}	1.91×10^{13}

Table 3 Natural and damped frequencies of the structure

	Soil type	ω	ω_1 (rad/s)	ω_2 (rad/s)	ω_3 (rad/s)
1	Soft soil	With damping	-0.02i ± 1.08	-0.24i ± 4.45	-0.62i ± 7.42
		Without damping	1.09	4.44	7.40
2	Medium soil	With damping	-0.02i ± 1.54	-0.21i ± 4.57	-0.58i ± 7.55
		Without damping	1.54	4.58	7.58
3	Dense soil	With damping	-0.02i ± 1.60	-0.21i ± 4.58	-0.58i ± 7.57
		Without damping	1.61	4.59	7.59
4	Fixed base	With damping	-0.03i ± 1.64	-0.21i ± 4.59	-0.58i ± 7.58
		Without damping	1.65	4.60	7.60

Table 4 The characteristics of earthquakes

No.	Earthquake	Date	Station	Time duration (s)	Maximum acceleration (m/s^2)	magnitude
1	Superstition hills	24 Nov 1987	Wildlife liquefaction array	45	2	6.3
2	San fernando	9 Feb 1971	LA - Hollywood stor lot	28	2.05	6.6
3	Northridge	17 Jan 1994	Canoga park - topanga canyon	40	2.25	6.7
4	Chi-Chi	20 Sep 1999	CHY101	90	3.45	7.6
5	El-Centro	18 May 1940	Imperial valley	40	3.5	7.1
6	Coyote lake	6 Aug 1979	Halls valley	40	0.5	5.7
7	Friuli	15 Sep 1976	Codroipo	33	0.3	5.7
8	N. Palm springs	8 July1986	Silent valley	24	1.35	6.0
9	Santa barbara	13 Aug 1978	Cachuma dam toe	12	0.71	6.0
10	Whittier narrows	4 Oct 1987	Mt wilson	40	1.21	5.3
11	Cape mendocino	25 April 1992	Eureka	44	1.75	7.1
12	Coalinga	2 May 1983	Parkfield	40	1.60	6.4
13	Imperial valley	15 Oct 1979	Delta	200	3.45	6.5
14	Landers	28 June 1992	Yermo fire station	44	2.40	7.3
15	Loma prieta	18 Oct 1989	Salinas - John & Work	40	1.10	6.9

The optimization program is performed on 2.8 GHz Core2Duo system with 4GB RAM. The consumed time is about an hour using 100 cycles for each earthquake data and soil type, and well convergence is achieved. However, the elapsed time is highly related to the amount of earthquake data (earthquake time steps) used in the program. The characteristics of all the earthquakes used in this paper are presented in Table 4.

5. Curve fitting

Using the ABC method, three sets of optimized parameters (μ , f and ξ) for each soil type and earthquake are obtained. For curve fitting, the following relation is considered for the mass ratio

$$\mu_{fit} = a_1 \mu_1^{n_1} + a_2 \mu_2^{n_2} \tag{13}$$

where

$$\mu_1 = \frac{M_{TMD}\,(fix\ based\ \ structure)}{M_s\,(fix\ based\ \ structure)} \tag{14a}$$

$$\mu_2 = \frac{M_s\,(fix\ based\ \ structure)}{M_s\,(structure\ with\ SSI)} \tag{14b}$$

$$M_s = \Phi^T [M] \Phi \tag{14c}$$

in which, Φ represents the normalized fundamental mode shape of the structure. In order to obtain the coefficients a_1, n_1, a_2 and n_2, the ABC method is utilized. In this case, the coefficients a_1, n_1, a_2 and n_2 are considered as the design variables, which are set as $0 \le a_1 , n_1 , a_2 , n_2 \le 5$. The objective is to minimize the Root Mean Square (RMS) of errors, which is defined in the following form

$$E(\mu) = \left[\frac{1}{N \times R} \sum_{i=1}^{N} \sum_{j=1}^{R} (\mu_{opt} - \mu_{fit})^2 \right]^{1/2} \tag{15}$$

where N and R represent the No. of earthquakes and soil types, respectively. The optimized values using the ABC method are obtained as follows

a_1= 1.1618

n_1= 1.3665

a_2= 0.5555

n_2= 0.3914

Fig. 3 represents the optimized and fitted values for the mass ratio. According to this figure, the structure constructed on the soil with greater stiffness and damping needs the TMD with smaller M_{TMD}. Considering Table 3, the soil with higher stiffness and damping brings higher natural and

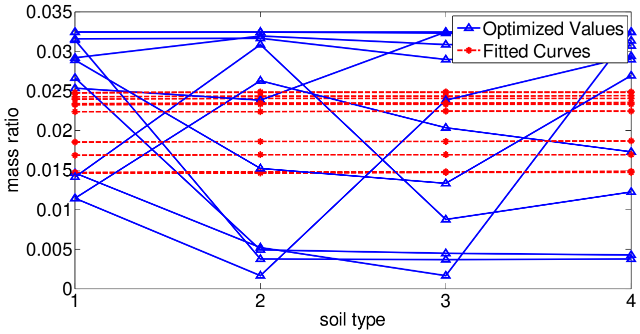

Fig. 3 Optimized and fitted values for mass ratio

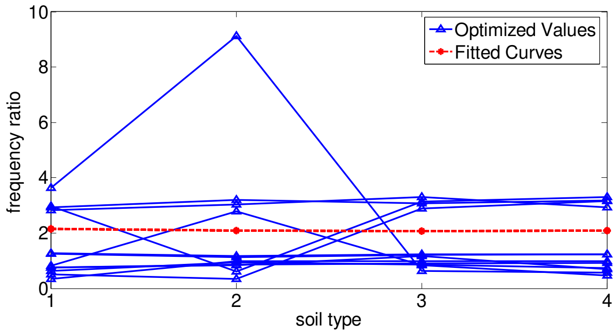

Fig. 4 Optimized and fitted values for the frequency ratio

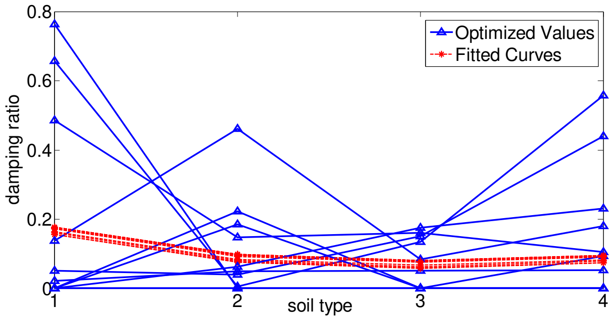

Fig. 5 Optimized and fitted values for damping ratio

damped frequency, therefore; it can be concluded that the structure with higher frequency (constructed on the dense soil) requires a TMD with lower mass ratio.

The similar method is employed to obtain the frequency ratio including the SSI effects, which is defined in the following form

$$f_{fit} = b_1 f_1^{m_1} + b_2 f_2^{m_2} \tag{16}$$

where

$$f_1 = \frac{1}{1+\mu\phi}\left[1-\beta\sqrt{\frac{\mu\phi}{1+\mu\phi}}\right] \tag{17a}$$

$$f_2 = \frac{C_s C_r}{K_s K_r} \tag{17b}$$

The parameters f_1 and ϕ shows the frequency ratio and the first modal participation factor for the fix based structure, respectively; and β represents the damping of the structure (Sadek *et al.* 1997). In order to find the best values of b_1, m_1, b_2 and m_2, these coefficients are assumed as the design variables ($0 \le b_1 , m_1 , b_2 , m_2 \le 5$), while the objective is to minimize the RMS of errors for frequency, which is calculated as follows

$$E(f) = \left[\frac{1}{N \times R}\sum_{i=1}^{N}\sum_{j=1}^{R}(f_{opt} - f_{fit})^2\right]^{1/2} \tag{18}$$

Using the ABC algorithm, the optimized values are achieved as follows

b_1= 2.1129

m_1= 0.7346

b_2= 3.7719

m_2= 0.6684

The optimized and fitted values for the frequency ratio are presented in Fig. 4. The results show that the structure constructed on the soil with greater stiffness and damping requires a TMD with smaller stiffness and natural frequency. According to Table 3, it can be seen that the structure with higher frequency (constructed on the dense soil) requires a TMD with lower natural frequency.

In order to reach the appropriate coefficients for the damping ratio considering the soil effects, the similar method is applied to the best values of damping ratio obtained by ABC method. The proposed relation for damping ratio is defined in the following form

$$\xi_{opt} = c_1\xi_1^{p_1} + c_2\xi_2^{p_2} \tag{19}$$

in which

$$\xi_1 = \phi\left[\frac{\beta}{1+\mu} + \sqrt{\frac{\mu}{1+\mu}}\right] \tag{20a}$$

$$\xi_2 = \frac{C_s C_r}{K_s K_r} \tag{20b}$$

The parameter ξ_1 shows the damping ratio for the fix based structure (Sadek *et al.* 1997). The

ABC method is employed to obtain the coefficients c_1, p_1, c_2 and p_2. Therefore, the mentioned coefficients are defined as the design variables, which are considered as $0 \le c_1, p_1, c_2, p_2 \le 5$. The objective function to be minimized is the RMS of errors, which is computed as follows

$$E(\xi)=\left[\frac{1}{N\times R}\sum_{i=1}^{N}\sum_{j=1}^{R}(\xi_{opt}-\xi_{fit})^2\right]^{1/2} \tag{21}$$

The optimized values for the design variables using the ABC method are obtained as follows

$$c_1 = 2.4426$$

$$p_1 = 2.6860$$

$$c_2 = 1.4953$$

$$p_2 = 0.4312$$

Fig. 5 shows the optimized and fitted values of damping ratio. The results show that there is a close relationship between the soil and optimized parameters of the TMD. According to this figure, the structure constructed on the soil with greater stiffness and damping needs a TMD with smaller damping coefficient. Therefore, the proper TMD for the dense soil is the one with lower ξ.

According to Table 3, the soil with higher stiffness and damping brings higher natural and damped frequency, therefore; it can be concluded that the structure with higher frequency requires TMD with lower damping ratio. The consumed time in this case is less than a minute using 1000 cycles for each fitting.

6. Results and discussions

The methodology outlined previously and the obtained relations are employed to design the TMD for the same structure with 10 different types of far field earthquakes, as presented in Table 4. By estimation of $\mu_1 = 3\%$, the real values of μ , f , ξ and therefore M_{TMD}, K_{TMD} and C_{TMD} are calculated for each soil type. The designed TMD is then employed to control the displacement and acceleration of the structure.

Figs. 6 and 7 show the displacement and acceleration reduction percentages for the mentioned earthquakes, respectively. According to Fig. 6, the maximum displacement is effectively reduced except for the structure on dense soil with Northridge oscillations. Fig. 7 illustrates that the designed TMD reasonably reduces the maximum acceleration of the structure. As it can be seen from these figures, the proposed relations result in acceptable reductions in most cases. However, there are some exceptions because the main purpose of the TMD design is the reduction of both acceleration and displacement in combined form, but not either of the two parameters separately.

The function reduction percentages for the mentioned earthquakes are presented in Fig. 8 for three soil types. It can be seen that the proposed relations result in effective reductions for all earthquakes and different soil types.

For further investigations, another 15 story structure is modeled and employed to design the TMD with the structural response calculated. The structure parameters are presented in Table 5

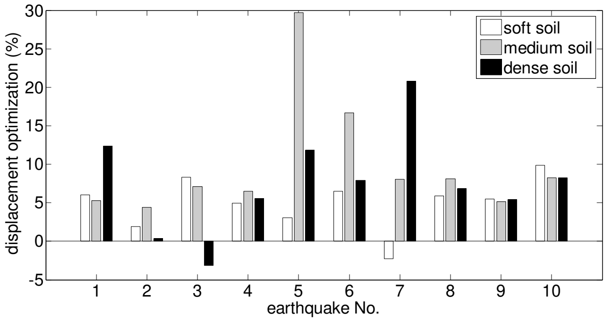

Fig. 6 The displacement reduction percentage

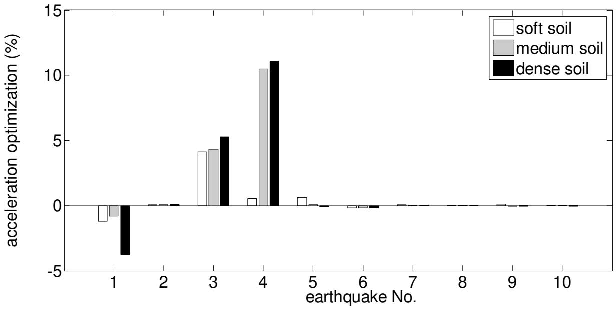

Fig. 7 The acceleration reduction percentage

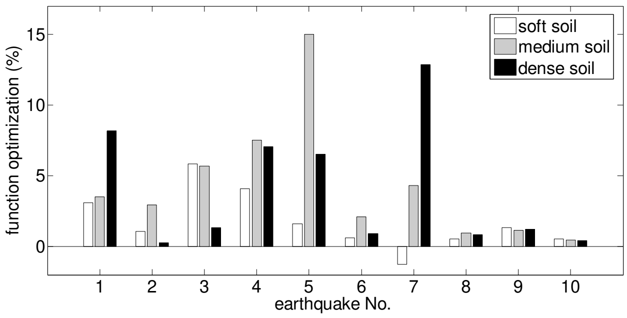

Fig. 8 The function reduction percentage

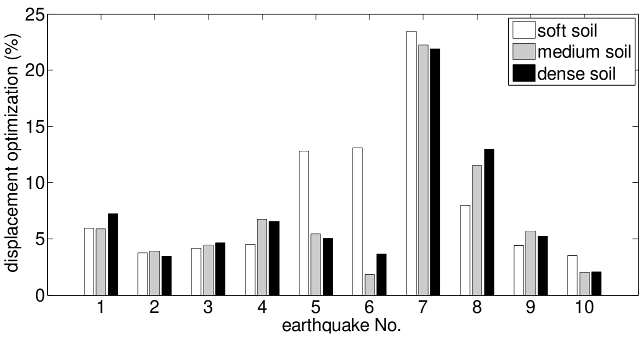

Fig. 9 The displacement reduction percentage

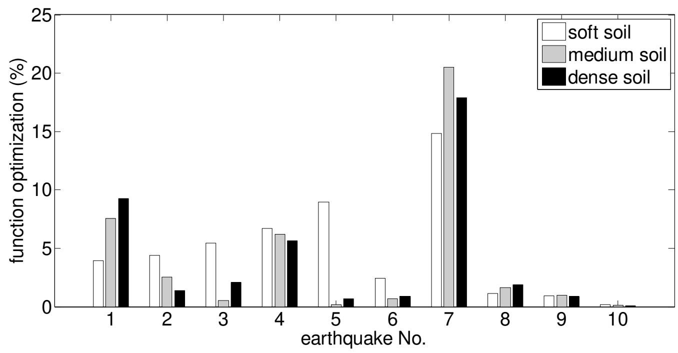

Fig. 10 The function reduction percentage

Table 5 Structure parameters (Guclu and Yazici 2008)

No. of stories	15
Story height (Z_i)	3.5 m
Story mass (M_i)	M_i = 3.456×10^5 kg M_1 = 4.500×10^5 kg
Story moment of inertia (I_i)	0.146×10^8 kgm^2
Story stiffness (K_i)	K_i = 3.40 × 10^8 N/m K_1=18.05 × 10^6 N/m
Foundation radius (R_0)	11.5 m
Foundation mass (M_0)	0.655 × 10^6 kg
Foundation moment of inertia (I_0)	0.220 × 10^8 kgm^2

Table 6 Natural and damped frequencies of the structure.

Soil type		ω	ω_1 (rad/s)	ω_2 (rad/s)	ω_3 (rad/s)
1	Soft soil	With damping	-0.004i ± 1.58	-0.08i ± 6.15	-0.08i ± 13.05
		Without damping	1.58	6.15	13.05
2	Medium soil	With damping	-0.002i ± 1.64	-0.03i ± 6.82	-0.08i ± 13.05
		Without damping	1.64	6.83	13.05
3	Dense soil	With damping	-0.002i ± 1.65	-0.02i ± 6.89	-0.08i ± 13.05
		Without damping	1.65	6.89	13.05
4	Fixed base	With damping	-0.002i ± 1.66	-0.02i ± 6.92	-0.08i ± 13.05
		Without damping	1.66	6.93	13.06

(Guclu and Yazici 2008). In this study, three types of ground properties, namely soft, medium and dense soil are examined, using the new soil parameters. Table 6 represents the first 3 natural and damped frequencies of the structure, considering and ignoring the SSI effects.

The previous methodology and the obtained relations are employed to design the TMD for controlling the new structure with 3 types of earthquakes. Estimating that $\mu_1 = 3\%$, the real values of μ, f, ξ and then M_{TMD}, K_{TMD} and C_{TMD} are calculated for each soil type.

The displacement reduction percentage for the mentioned earthquakes is presented in Fig. 9. This figure reveals that the designed TMD can effectively reduce the maximum displacement of the structure. Further studies reveal that the maximum acceleration is reasonably reduced except in few cases, mainly due to the fact that the main purpose of TMD design is to reduce the combination of acceleration and displacement, and not either the two parameters separately. However, the proposed relations result in acceptable reductions in most cases.

The function reduction percentage for the mentioned earthquakes is presented in Fig. 10. It can be seen that the proposed relations result in effective reductions for all earthquakes and different soil types. As it can be seen from Figs. 6-10, the reduction percentage is higher for El-Centro and Friuli earthquakes in most cases. This is mainly because one of the principal frequencies of the mentioned earthquakes are completely near the tuned frequency of TMD. However, further structure samples and earthquakes are to be investigated for the better estimation of TMD parameters.

7. Conclusions

In this paper, the ABC technique is utilized to modify the former relations for the optimized TMD parameters considering the soil effects. A 40 story structure with three soil types is employed to design the TMD in order to control both the displacement and acceleration for five types of far field earthquakes. The results are then employed to obtain relations for the optimized TMD parameters with SSI effects. The relations are employed to design TMD for the same structure with another three types of far field oscillations, and reasonable results are achieved. For further investigations, the obtained relations are utilized to design the TMD for a new structure, and the reduction values are obtained for 10 new types of earthquakes, which show acceptable results. This study improves the understanding of earthquake oscillations, and helps the designers achieve the optimized TMD for controlling the vibrations of high-rise buildings.

Acknowledgements

This work was supported by Research Grant No. 2/18192 from Ferdowsi University of Mashhad, Mashhad, Iran.

References

Averill, F.W., Morris, J.R. and Cooper, V.R. (2009), "Calculated properties of fully hydrogenated single layers of BN, BC2N, and graphene: graphene and its BN-containing analogues", *Phys. Rev. B*, **80**, 195411.

Dodziuki, H. (2005), "Modeling complexes of H2 molecules in fullerenes", *Chem. Phys. Lett.*, **410**, 39-41.

Ding, F., Lin, Y., Krasnov, P.O. and Yakobson, B.I. (2007), "Nanotube-derived carbon foam for hydrogen sorption", *J. Chem. Phys.*, **127**, 164703.

Dresselhaus, M.S., Dresselhaus, G. and Eklund, P.C. (1996), *Science of Fullerenes and Carbon Nanotubes*, Academic Press, San Diego, CA, USA.

Drexler, K.E. (1992), *Nanosystems – Molecular Machinery*, Manufacturing and Computation, John Wiley & Sons, New York, USA.

Er, S., Wijs de, G.A. and Brocks, G. (2009), "Hydrogen storage by polylithiated molecules and nanostructures", *J. Phys. Chem. C*, **113**(20), 8997-9002.

Holbrook, K.A., Pilling, M.J. and Robertson, S.H. (1996), *Unimolecular Reactions*, John Wiley & Sons,

New York, USA.
Kim, B.R., Pyo, S.H., Lemaire, G. and Lee, H.K. (2011), "Multiscale approach to predict the effective elastic behavior of nanoparticle-reinforced polymer composites", *Interact. Multiscale Mech.*, **4**, 173-185.
Kruse, H. and Grimme, S. (2009), "Accurate Quantum Chemical Description of Non-Covalent Interactions in Hydrogen Filled Endohedral Fullerene Complexes", *J. Phys. Chem.C*, **113**, 17006-17010.
Labet, V., Gonzalez-Morelos, P., Hoffmann, R. and Ashcroft, N.W. (2012), "A fresh look at dense hydrogen under pressure. I. An introduction to the problem, and an index probing equalization of H-H distances", *J. Chem. Phys.*, **136**, 074501.
Lachawiec, A.J., Qi, G. and Yang, R.T. (2005), "Hydrogen storage in nanostructured carbons by spillover: bridge-building enhancement", *Langmuir*, **21**, 11418-11424.
Lee, T.B. and McKee, M.L. (2008), "Endohedral hydrogen exchange reactions in C60 (nH2@C60, n=1-5): comparison of recent methods in a high-pressure cooker", *J. Am. Chem. Soc.*, **130**, 17610-17619.
Li, R. and Sun, L.Z. (2011), "Dynamic mechanical analysis of silicone rubber reinforced with multi-walled carbon nanotubes", *Interact. Multiscale Mech.*, **4**, 239-245.
Li, Y. and Yang, R.T. (2006), "Significantly enhanced hydrogen storage in metal-organic frameworks via spillover", *J. Am. Chem. Soc. JACS Commun.*, **128**, 726-725.
Lin, Y., Ding, F. and Yakobson, B.I. (2008), "Hydrogen storage by spillover on graphene as a phase nucleation process", *Phys. Rev. B*, **78**, 041402.
Liu, W., Zhao, Y.H., Li, Y., Jiang, Q. and Lavernia, E.J. (2009), "Enhanced hydrogen storage on Li-dispersed carbon nanotubes", *J. Phys. Chem. C*, **113**, 2028-2033.
Mattesini, M., Soler, J.M. and Yndurain, F. (2006), "Ab initio study of metal-organic framework-5 Zn_4O(1,4-benzenedicarboxylate)$_3$: an assessment of mechanical and spectroscopic properties", *Phys. Rev. B*, **73**, 094111.
Bockman, T.M., Hubig, S.M. and Kochi, J.K. (1996), "Direct observation of carbon-carbon bond cleavage in ultrafast decarboxylations", *J. Am. Chem. Soc.*, **119**, 4502-4503.
Miller, G.P., Kintigh, J., Kim, E., Weck, P.F., Berber, S. and Tomanek, D. (2008), "Hydrogenation of single-wall carbon nanotubes using polyamine reagents: combined experimental and theoretical study", *J. Am. Chem. Soc.*, **130**, 2296-2303.
Pupysheva, O.V., Farajian, A.A. and Yakobson, B.I. (2008), "Fullerene nanocage capacity for hydrogen storage", *Nano Lett.*, **8**, 767-774.
Salam, M.A., Sufian, S. and Lwin, Y. (2013), "Hydrogen adsorption study on mixed oxides using the density functional theory", *J. Phys. Chem. Solids*, **74**, 558-564.
Shen, L. (2013), "Molecular dynamics study of Al solute-dislocation interactions in Mg alloys", *Interact. Multiscale Mech.*, **6**, 127-136.
Singh, A.K., Ribas, M.A. and Yakobson, B.I. (2009), "H-spillover through the catalyst saturation: an ab initio thermodynamics study", *ACS Nano*, **3**, 1657-1662.
Sofo, J.O., Chaudhari, A.S. and Barber, G.D. (2007), "Graphane: a two-dimensional hydrocarbon", *Phys. Rev. B*, **75**, 153401.
Soler, J.M., Artacho, E., Gale, J.D., Garcia, A., Junquera, J., Ordejon, P. and Sanchez-Portal, D. (2002), "The SIESTA method for ab initio order-N materials simulation", *J. Phys. Cond. Mat.*, **14**, 2745-2779.
Stadie, N.P., Purewal, J.J., Ahn, C.C. and Fultz, B. (2010), "Measurements of hydrogen spillover in platinum doped superactived carbon", *Langmuir*, **26**, 15481-15485.
Strobel, R., Garche, J., Moseley, P.T., Jorissen, L. and Wolf, G. (2006), "Hydrogen storage by carbon materials", *J. Power Sources*, **159**(2), 781-801.
Tsetseris, L. and Pantelides, S.T. (2012), "Hydrogen uptake by graphene and nucleation of graphane", *J. Mater. Sci.*, **47**(21), 7571-7579.
Tukerman, M.E. (2010), *Statistical Mechanics: Theory and Molecular Simulation*, Oxford University Press, Oxford, UK.
Wang, Q., Sun, Q., Jena, P. and Kawazoe, Y. (2009), "Theoretical study of hydrogen storage in Ca-coated fullerenes", *J. Chem. Theory Comput.*, **5**, 374-379.
Wang, X. and Lee, J.D. (2011), "Heat resistance of carbon nanoonions by molecular dynamics simulation",

Interact. Multiscale Mech., **4**, 247-255.
Wen, X.D., Yang, T. and Hoffmann, R., Ashcroft, N.W., Martin, R.L., Rudin, S.P. and Zhu, J.X. (2012), "Graphane nanotubes", *ACS Nanos*, **6**, 7142-7150.
Wu, G., Wang, J., Zeng, X.C., Hu, H. and Ding, F. (2010), "Controlling cross section of carbon nanotubes via selective hydrogenation", *J. Phys. Chem. C.*, **114**, 11753-11757.